

Climate of the past

Supporting Information for

Holocene fire regimes around the Altai-Sayan Mountains and adjacent plains: interaction with climate and vegetation types

Dongliang Zhang^{1,2,3,*}, Blyakharchuk Tatiana⁴, Aizhi Sun⁵, Xiaozhong Huang⁶, Yuejing Li^{1,2,3}

¹ *State Key Laboratory of Ecological Safety and Sustainable Development in Arid Lands, Xinjiang Institute of Ecology and Geography, Chinese Academy of Sciences, 818 Beijing South Road, Urumqi 830011, China.*

² *Research Center for Ecology and Environment of Central Asia, Chinese Academy of Sciences, 818 Beijing South Road, Urumqi 830011, China.*

³ *University of Chinese Academy of Sciences, 19A Yuquan Road, Beijing 100049, China.*

⁴ *Institute of Monitoring of Climatic and Ecological Systems, Siberian Branch of Russian Academy of Sciences, Tomsk, Russia.*

⁵ *College of Earth and Planetary Sciences, University of Chinese Academy of Sciences, Beijing 100049, China.*

⁶ *College of Earth and Environmental Sciences, Lanzhou University, Lanzhou, China.*

* Corresponding author.

E-mail address: zhdl@ms.xjb.ac.cn

This PDF file includes:

Text S1

Figures S1 to S8

Text S1—Biomass burning-vegetation relationships at the selected sites

In the southeast/west Altai Mountains within the steppe zone (Region A):

Tolbo Lake: In the early Holocene, the charcoal influx was in the relatively high level with a average of 174.98 particles/cm²/yr. Three peaks were observed at ~11.08, ~10.15, ~8.56 cal. kyr BP with the highest value of 757.07 particles/cm²/yr (Fig. 4) (Hu et al., 2024). The relatively low charcoal influx was showed between ~8.2 and ~6 cal. kyr BP with a average of 59.86 particles/cm²/yr. After ~6 cal. kyr BP, the charcoal influx shows an increasing trend with abnormal high value at ~1.20~0.65 cal. kyr BP. Biomass burning significantly increases with increasing *Pinus* (p=0.00) and primary forest cover (p=0.00), whereas that significantly increases with decreasing *Picea* abundance (p=0.002) and forest density (p=0.00) (Table S2). *Betula* (p=0.09), *Larix* (p=0.95) abundance had insignificant effects on biomass burning (Table S2, Fig. S1).

Alahake Lake: the charcoal influx was in the relatively low level with a average of 0.64 particles/cm²/yr before ~1.44 cal. kyr BP, followed by an abrupt increase of charcoal influx at ~1.44~1.02 cal. kyr BP with a relatively low value in the remaining interval (Li et al., 2021). In the past millennium, two peaks were showed at ~0.74~0.67 cal. kyr BP and ~0.45~0.37 cal. kyr BP (Fig. 2b). Only *Betula* (p=0.04) abundance had significant effects on biomass burning. Biomass burning insignificantly increases with *Abies* (p=0.45), *Larix* (p=0.19), *Picea* (p=0.09), *Pinus* (p=0.089), and primary cover (p=0.26) (Table S2, Fig. S1).

Kuchuk Lake: The obviously increased charcoal influx was occurred in the past 1500 years (Fig. 4b). The GAMs analysis reveals that *Abies* (p=0.03), *Betula* (p=0.00) and *Pinus sylvestris* (p=0.01) have significant positive relationship with biomass burning at Kuchuk Lake with the highest 25.5% explained deviance (Table S2, Fig. S2). Biomass burning of Kuchuk Lake clearly reflected “human influence charcoal pulse” during last two millennium.

In the west Siberian plain (Region B, n=4):

Rybnaya Mire: Three high-value interval of charcoal influx occurred at ~7.45~6.85 cal. kyr BP, ~6.35~6.2 cal. kyr BP and ~4.5~4.3 cal. kyr BP (Fig. 4c). The

GAMs analysis reveals that biomass burning significantly decreases with increasing *Betula* ($p=0.004$, 18.4%) and primary cover ($p=0.003$, 16.2%), whereas that significantly decreases with decreasing *Picea* abundance ($p=0.00$, 44.5%) (Table S2, Fig. S2).

Plotnikovo Mire: two high-value interval of charcoal influx occurred at ~1.58-~0.98 cal. kyr BP and the past 350 years (Fig. 4c). The GAMs analysis reveals that only primary forest cover have significant positive relationship ($p=0.004$) with biomass burning with the 39.70% deviance explanation (Table S2, Fig. S2). Other variables have no significant relationships with biomass burning.

Shchuchye Lake: the highest charcoal influx (mean 4431.03 particles/cm²/yr) was observed at ~12~11.34 cal. kyr BP (Fig. 4c). The following interval (~11.34~4.91 cal. kyr BP) was featured by the relatively low charcoal influx with an average of 787.31 particles/cm²/yr. Increasing charcoal influx (mean 1481.92 particles/cm²/yr) was observed in the past ~4900 years. The GAMs analysis reveals that all variables have significant relationships with biomass burning in Shchuchye Lake (Table S2, Fig. S3). The higher explained deviance for biomass burning was presented in primary forest cover (57.4%), *Larix* (45.4%) and *Abies* (37.4%).

Ulukh–Chayakh Mire: the charcoal influx was relatively stable with four peaks at ~4.37~4.21 cal. kyr BP, ~3.73~2.88 cal. kyr BP, ~0.97~0.92 cal. kyr BP and the past 300 years (Fig. 4c). Biomass burning significantly increases with increasing *Betula* ($p=0.01$, 13.4%), whereas that significantly increases with decreasing *Pinus sylvestris* abundance ($p=0.04$, 10.3%) (Table S2, Fig. S3). Other variables (*Abies*, *Betula*, *Larix*, *Picea*, *Pinus sibirica* and primary forest cover) has no significant relationships with biomass burning.

In the northern Altai Mountains (Region C, n=4):

Chudnoye Mire: the charcoal influx experienced a decreasing trend in the early and middle Holocene and turned to a quick increase (mean 1497.13 particles/cm²/yr) in the late Holocene (Fig. 4c). The GAMs analysis reveals that only *Abies* pollen ($p=0.14$) and primary forest cover ($p=0.17$) have no relationship with biomass burning (Table S2, Fig. S3). *Betula*, *Larix*, *Picea*, *Pinus sibirica*, *Pinus sylvestris* have

significant relationships with biomass burning. The high explained deviance for biomass burning was presented in *Picea* (30.3%) and *Betula* (23.5%).

Tundra Mire: the charcoal influx decreased from 437.97 to 66.42 particles/cm²/yr at ~7.28~4.41 cal. kyr BP and increased to 1056.34 particles/cm²/yr at ~4.41~2 cal. kyr BP. The charcoal influx experienced a slow decrease at ~2~1.65 cal. kyr BP, a quick increase at ~1.65~0.88 cal. kyr BP with the highest value (3177.54 particles/cm²/yr) at ~1.42~1.32 cal. kyr BP and again a slow decrease in the remaining interval (Fig. 4c). The GAMs analysis reveals that only *Larix* pollen have significant positive relationship with biomass burning with the 22.70% deviance explanation (Table S2, Fig. S4). Other variables (*Abies*, *Betula*, *Picea*, *Pinus sibirica*, *Pinus sylvestris* and primary forest cover) has no significant relationships with biomass burning.

Mokhovoe Bog: the charcoal influx in the Holocene interval can be divided into three parts: a slow decrease in the early Holocene, an abrupt increase at ~8.2 cal. kyr BP followed by a decrease at ~8.2~6 cal. kyr BP. A quick increase of charcoal influx was also occurred at ~5.5~4.2 cal. kyr BP with a following decreasing trend in the remaining interval. Six peaks of charcoal influx were showed at ~8.30, ~8.07, ~5.40, ~4.81, ~4 and ~1.42 cal. kyr BP (Fig. 4c). The GAMs analysis reveals that only *Picea* pollen (p=0.02) have significant relationship with biomass burning at Mokhovoe Bog with 11.9% explained deviance (Table S2, Fig. S4).

Kuatang Lake: the charcoal influx kept a relatively low level with an average of 236.26 particles/cm²/yr between ~5.87 and ~3.73 cal. kyr BP (Fig. 4c). The following interval was featured by the relatively high level with an average of 983.01 particles/cm²/yr at ~3.73~1.78 cal. kyr BP. The charcoal influx turned to the lower level in the next 1200 years and again increased in the past 500 years. The GAMs analysis reveals that biomass burning significantly increases with increasing *Betula* (p=0.00), *Pinus sibirica* (p=0.05), *Pinus sylvestris* (p=0.02) pollen and primary forest cover percentage (p=0.003), whereas that significantly increases with decreasing *Abies* (p=0.04). *Larix* and *Picea* have no significant relationship with biomass burning (Table S2, Fig. S4).

The central Altai Mountains within the forest zone (Region D, n=3):

Dzhangyskol Lake: there are two high-value interval of charcoal influx at ~12~10 cal. kyr BP (3.88 particles/cm²/yr) and the last millennium (8.10 particles/cm²/yr) (Fig. 4e). The remaining interval (~10~1 cal. kyr BP) was characterized by a low value (1.08 particles/cm²/yr) with a slight increasing trend of charcoal influx. The GAMs analysis reveals that all variables have no significant relationships with biomass burning (Table S2, Fig. S5). *Pinus sylvestris* has the largest deviance explanation (22.80%) for biomass burning with a positive relationship.

Uzunkol Lake: the charcoal influx was lower with an average of 46.16 particles/cm²/yr before ~4.76 cal. kyr BP with an abnormally peak (531.78 particles/cm²/yr) at ~9.18 cal. kyr BP (Fig. 4e). Between ~4.76 and ~1.25 cal. kyr BP, the charcoal influx obviously increased with an average of 93.13 particles/cm²/yr. The maximum charcoal influx (mean 244.67 particles/cm²/yr) was recorded in the past ~1.25 cal. kyr BP with a quick decreasing trend. The GAMs analysis reveals that biomass burning significantly increases with increasing *Abies* (p=0.02) and *Pinus sylvestris* (p=0.02) percentage, whereas that significantly increases with decreasing *Betula* (p=0.008), *Picea* (p=0.00) and *Larix* (p=0.00). *Pinus sibirica* and primary forest cover has no significant relationships with biomass burning (Table S2, Fig. S5).

Kendegelukol Lake: the charcoal influx was lower (mean 16.23 particles/cm²/yr) at ~12~10 cal. kyr BP and turns the higher level in the remaining interval with two peaks at ~4.16~3.65 cal. kyr BP (mean 349.79 particles/cm²/yr) and ~1.45~1.30 cal. kyr BP (mean 199.35 particles/cm²/yr) (Fig. 4e). The GAMs analysis reveals that biomass burning significantly increases with increasing *Abies* (p=0.04), *Betula* (p=0.02), *Pinus sylvestris* (p=0.00) pollen with >40% explained deviance. Other variables (*Larix*, *Picea*, *Pinus sibirica* and primary forest cover) has no significant relationships with biomass burning (Table S2, Fig. S5).

The central Altai Mountains above the forest limit (Region E, n=3):

Akkol Lake: the charcoal influx can be divided into four intervals: a lower interval at ~12~10 cal. kyr BP, the maximum interval at ~10~5 cal. kyr BP, a lowing interval at ~5~2 cal. kyr BP and a slight increasing interval in the past two

millennium (Fig. 4f). The GAMs analysis reveals that biomass burning significantly decreases with decreasing *Picea* ($p=0.00$), *Pinus sylvestris* ($p=0.002$) and primary forest cover ($p=0.00$) (Table 2). Other variables (*Abies*, *Betula*, *Larix*, *Pinus sibirica*) has no significant relationships with biomass burning (Table S2, Fig. S6).

Tashkol Lake: the highest charcoal influx was showed at ~12~10 cal. kyr BP. The increasing trend of charcoal influx was showed before ~5.5 cal. kyr BP, followed by a decreasing trend in the remaining interval (Fig. 4f). The GAMs analysis reveals that biomass burning significantly decreases with decreasing *Picea* pollen ($p=0.04$) with 40.7% explained deviance (Table S2). The second higher explained deviance (17%) for biomass burning was primary forest cover, but no significance was recorded in Tashkol Lake. The explained deviance of other variables (*Abies*, *Betula*, *Larix*, *Pinus sibirica*, *Pinus sylvestris* and primary forest cover) are less than 5% (Table S2, Fig. S6).

Grusha Lake: the charcoal influx show a decreasing trend from 48.64 to 7.77 particles/cm²/yr since late glacial to ~1.6 cal. kyr BP and followed by a slow increase in the remaining interval (Fig. 4f). The GAMs analysis reveals that biomass burning significantly decreases with decreasing *Larix* ($p=0.02$), *Picea* ($p=0.05$) and primary forest cover ($p=0.00$) with the largest deviance explanation (71.10%) (Table S2). Other variables in Akkol Lake (*Abies*, *Betula*, *Pinus sibirica* and *Pinus sylvestris*) has no significant relationships with biomass burning (Table S2, Fig. S6).

The Western Sayan Mountains (Region F, n=3):

Bezrybnoye Mire (within mountain forest upper limit): the charcoal influx show a quick increase from 449.95 to 2691.87 particles/cm²/yr at ~4~5 cal. kyr BP and experienced a quick decrease in the late Holocene (Fig. 4g). The GAMs analysis reveals that all variables has no significant relationships with biomass burning (Table S2, Fig. S7). *Pinus sylvestris* had the largest deviance explanation (28.10%) for biomass burning with a negative relationship.

Buibinskoye Mire (within mountain forest upper limit): the charcoal influx show a quick increase from 1581.52 to 10765.67 particles/cm²/yr in the early Holocene and experienced a quick decrease from 10765.67 to 210.43 particles/cm²/yr

in the middle and late Holocene (Fig. 4g). The GAMs analysis reveals that biomass burning significantly decreases with decreasing *Abies* ($p=0.004$) pollen percentage (Table 2). Other variables (*Betula*, *Larix*, *Picea*, *Pinus sibirica*, *Pinus sylvestris* and primary forest cover) has no significant relationships with biomass burning (Table S2, Fig. S7).

Lugovoe Mire (within mountain forest): the charcoal influx significantly decreased from 1338.64 to 19.07 particles/cm²/yr at ~7.7~1.18 cal. kyr BP and turned to a quick increase to 837.66 particles/cm²/yr in the remaining interval (Fig. 4g). The GAMs analysis reveals biomass burning significantly decreases with decreasing *Abies* ($p=0.02$) and *Larix* ($p=0.008$) pollen percentage, whereas that significantly decreases with increasing *Pinus sylvestris* pollen ($p=0.01$) (Table S2). Other variables (*Betula*, *Picea*, *Pinus sibirica*, forest density and primary forest cover) has no significant relationships with biomass burning (Table S2, Fig. S7).

The Khangai Mountains (Region G, n=3):

Olgi Lake: the charcoal influx was relatively low in the whole interval with an average of 9.19 particles/cm²/yr and one peak (88.28 particles/cm²/yr) primary forest cover appeared at ~3.5~3.1 cal. kyr BP (Fig. 4h). Biomass burning significantly correlates with *Betula* ($p=0.02$), *Larix* ($p=0.03$), *Picea* ($p=0.003$), *Pinus* ($p=0.00$) and primary forest cover ($p=0.00$) (Table S2, Fig. S8).

Shireet Naiman Nuur: the charcoal influx experienced a decreasing trend in the past 7600 years with two peaks at ~6.9~6.7 cal. kyr BP and ~3.7~3.3 cal. kyr BP (Fig. 4h). The GAMs analysis reveals that all variables has significant relationships with biomass burning (Table S2, Fig. S8). Primary forest cover (37.4%), *Pinus sibirica* (27.5%) and *Betula* (20.7%) had the larger deviance explanation for biomass burning with a positive relationship.

Ugii Nuur: the charcoal influx had two peaks at ~8.46~7.49 cal. kyr BP and ~2.44~2.12 cal. kyr BP (Fig. 4h). The value of charcoal influx in the latter period (mean 1644.66 particles/cm²/yr) is totally higher than that in the former interval (mean 689.61 particles/cm²/yr). The GAMs analysis reveals *Larix* ($p=0.00$), *Pinus sibirica* ($p=0.00$) and primary forest cover ($p=0.00$) has significant relationships with biomass

204 burning (Table S2, Fig. S8), while *Betula* ($p=0.06$) and *Picea* ($p=0.67$) has
205 insignificant relationships with biomass burning.
206

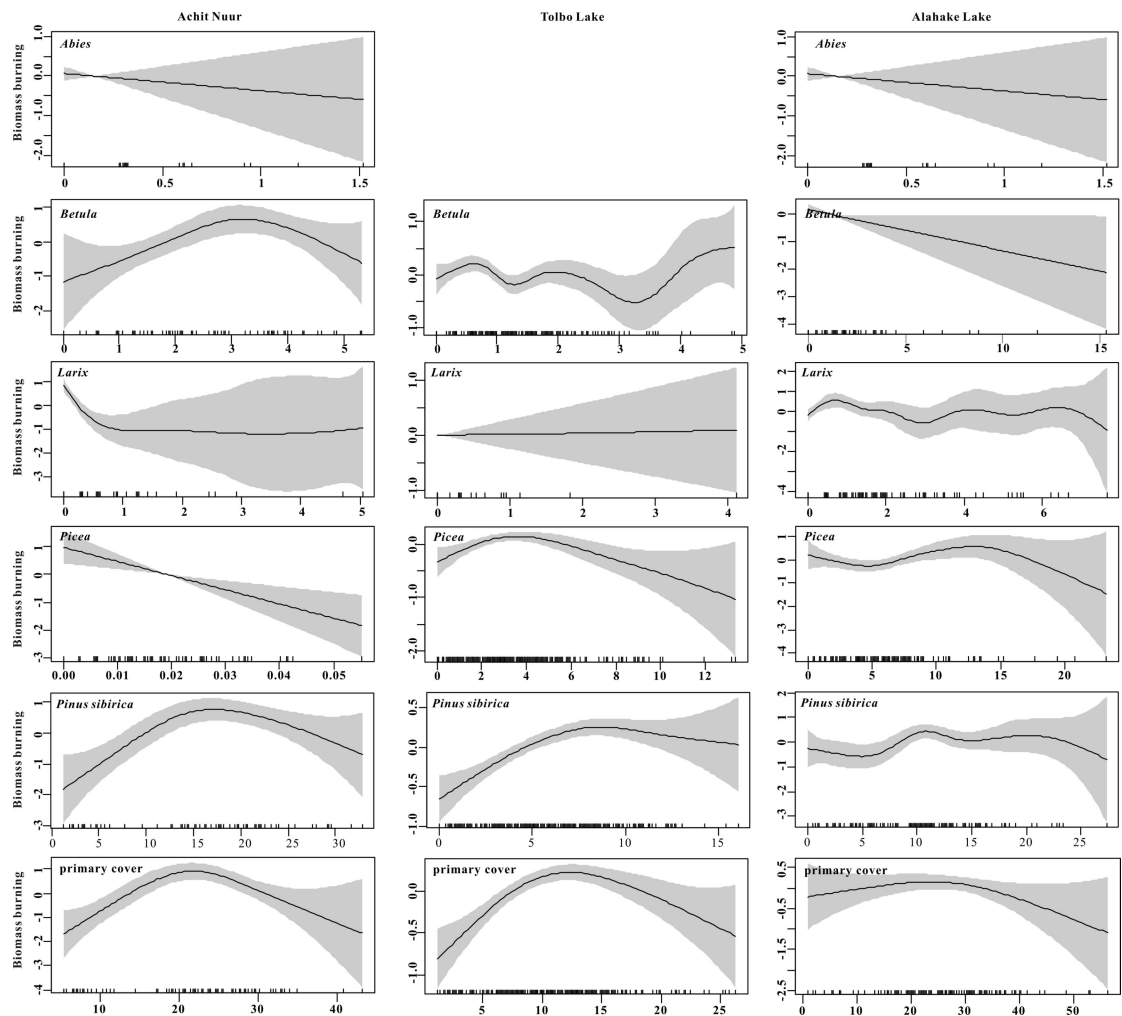


Fig. S1. Generalized Additive Models showing the relationship between biomass burning (y-axis) and dominant drivers (*Abies*, *Betula*, *Larix*, *Picea*, *Pinus sibirica* and primary forest cover) in Achit Nuur, Tolbo Lake and Alahake Lake. Pointwise confidence intervals (95%) are indicated by the gray bands.

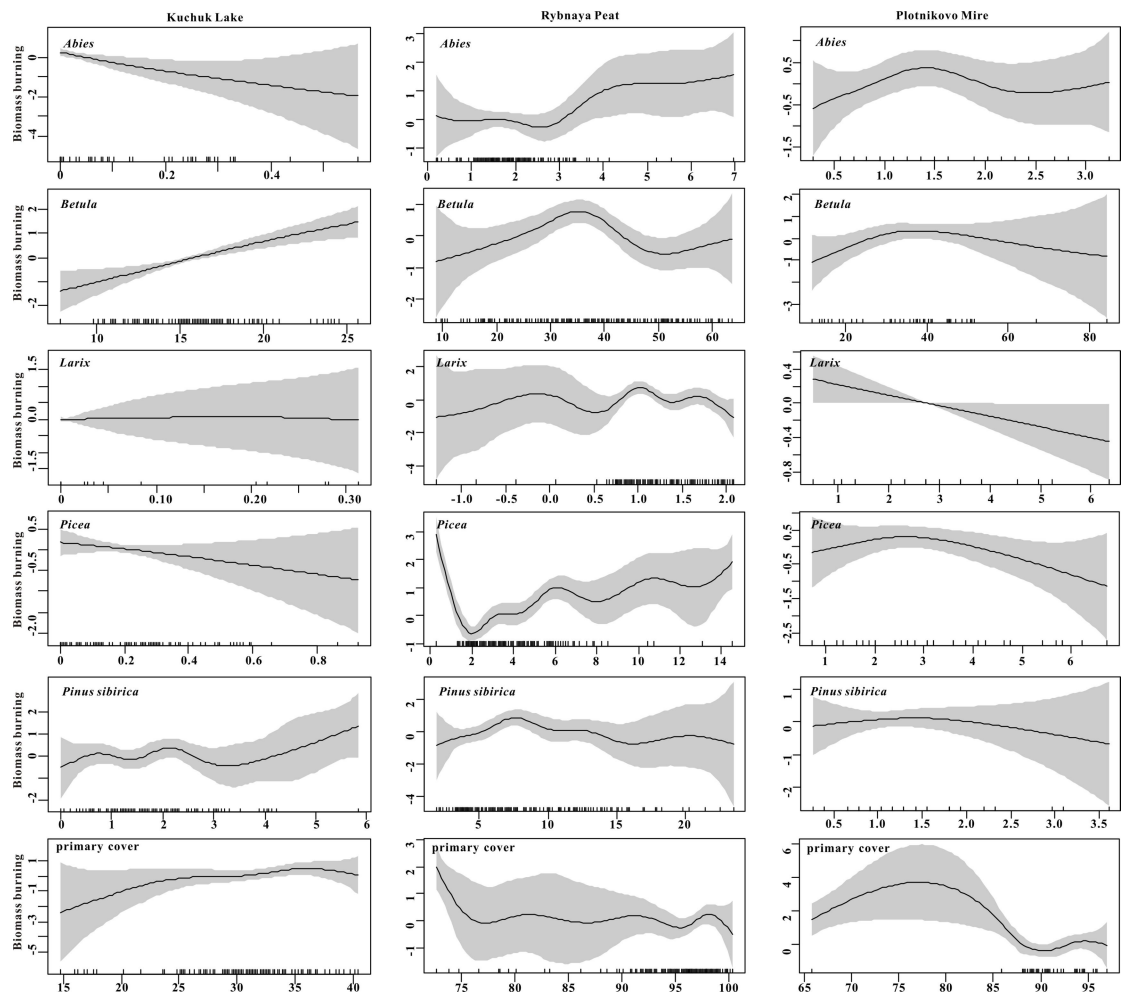


Fig. S2. Generalized Additive Models showing the relationship between biomass burning (y-axis) and dominant drivers (*Abies*, *Betula*, *Larix*, *Picea*, *Pinus sibirica* and primary forest cover) in Kuchuk Lake, Rybnaya Mire and Plotnikovo Mire. Pointwise confidence intervals (95%) are indicated by the gray bands.

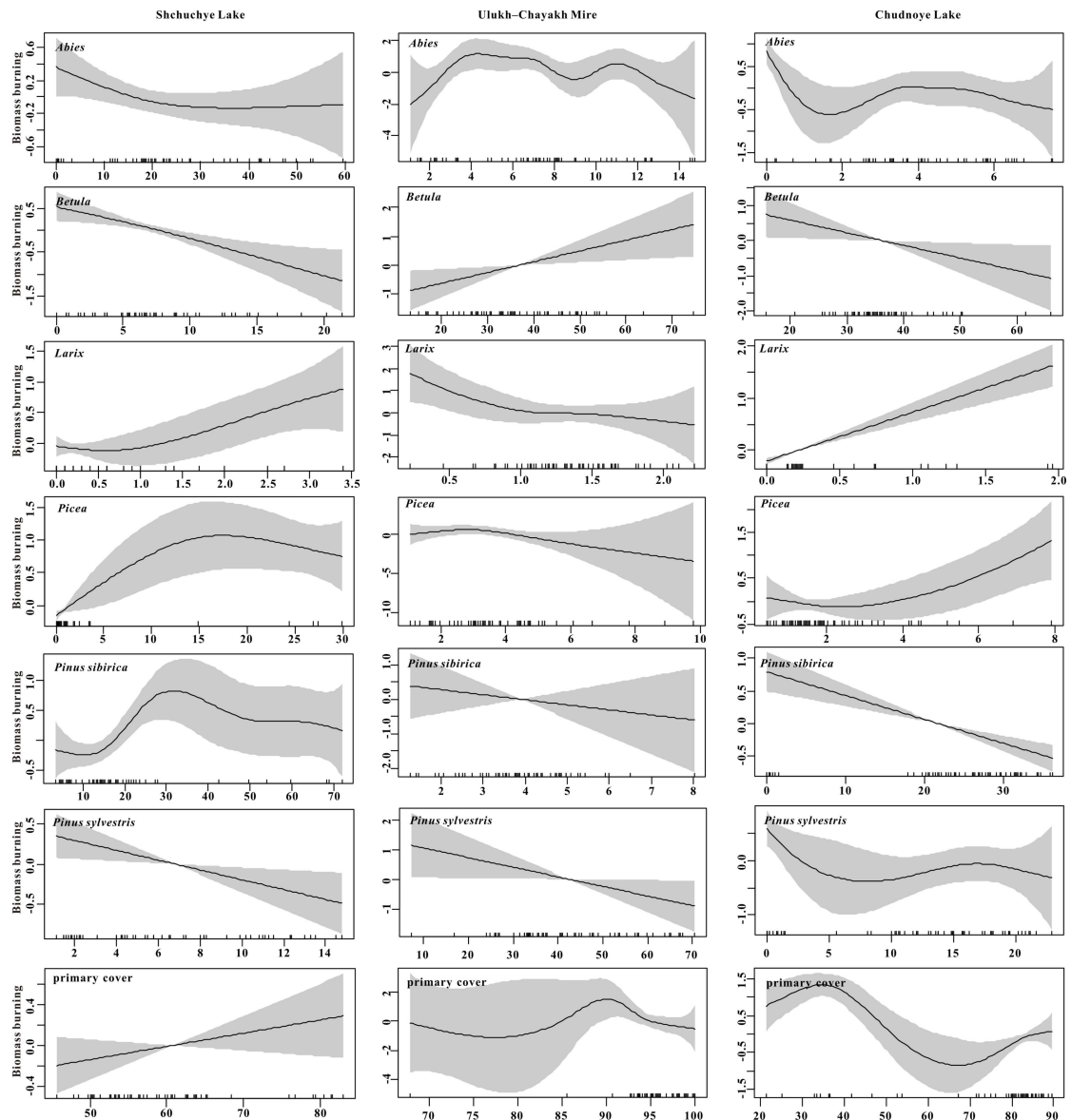


Fig. S3. Generalized Additive Models showing the relationship between biomass burning (y-axis) and dominant drivers (*Abies*, *Betula*, *Larix*, *Picea*, *Pinus sibirica*, *Pinus sylvestris* and primary forest cover) in Shchuchye Lake, Ulukh-Chayakh Mire and Chudnoye Mire. Pointwise confidence intervals (95%) are indicated by the gray bands.

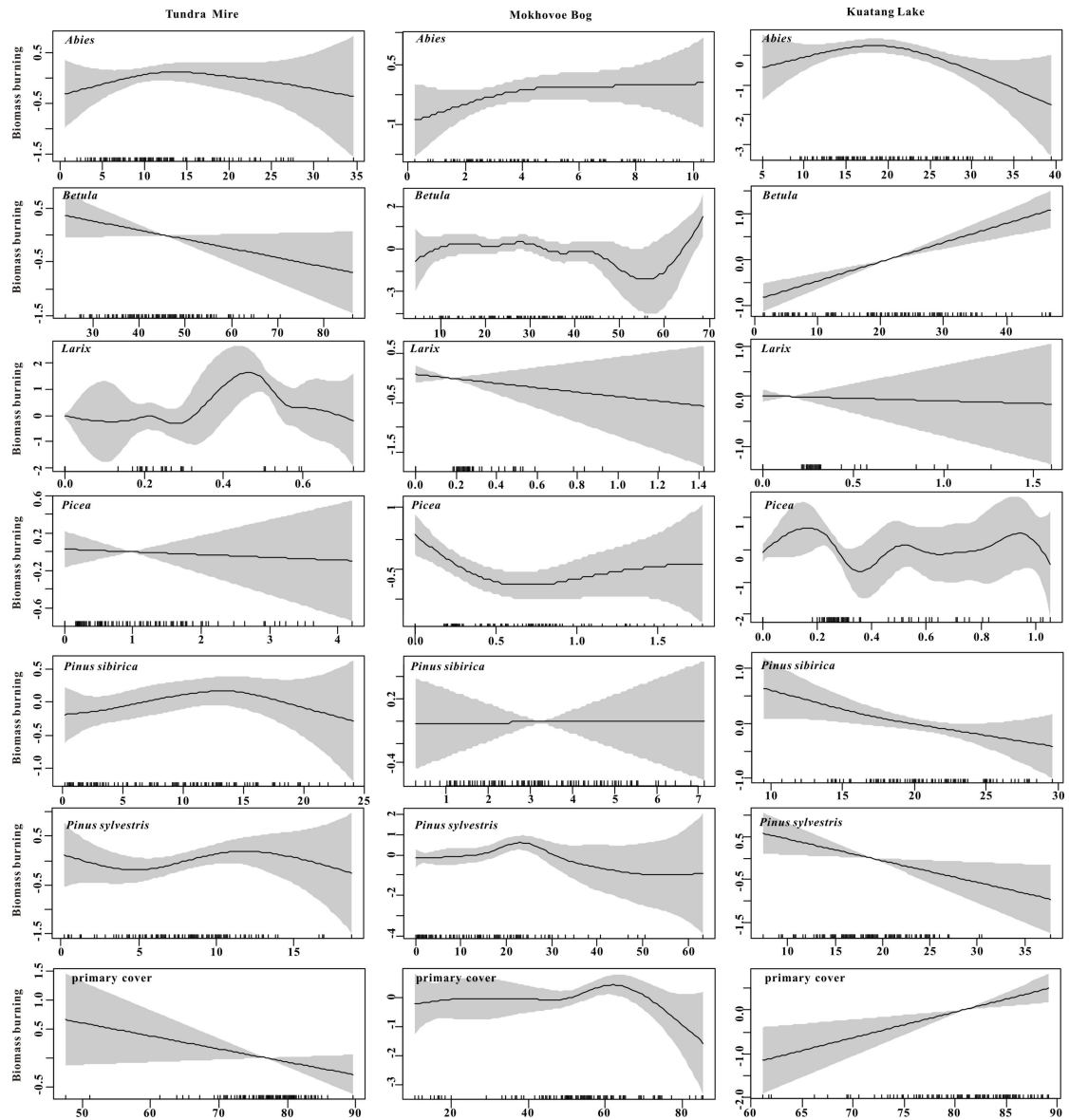


Fig. S4. Generalized Additive Models showing the relationship between biomass burning (y-axis) and dominant drivers (*Abies*, *Betula*, *Larix*, *Picea*, *Pinus sibirica*, *Pinus sylvestris* and primary forest cover) in Tundra Mire, Mokhovoe Bog and Kuantang Mire. Pointwise confidence intervals (95%) are indicated by the gray bands.

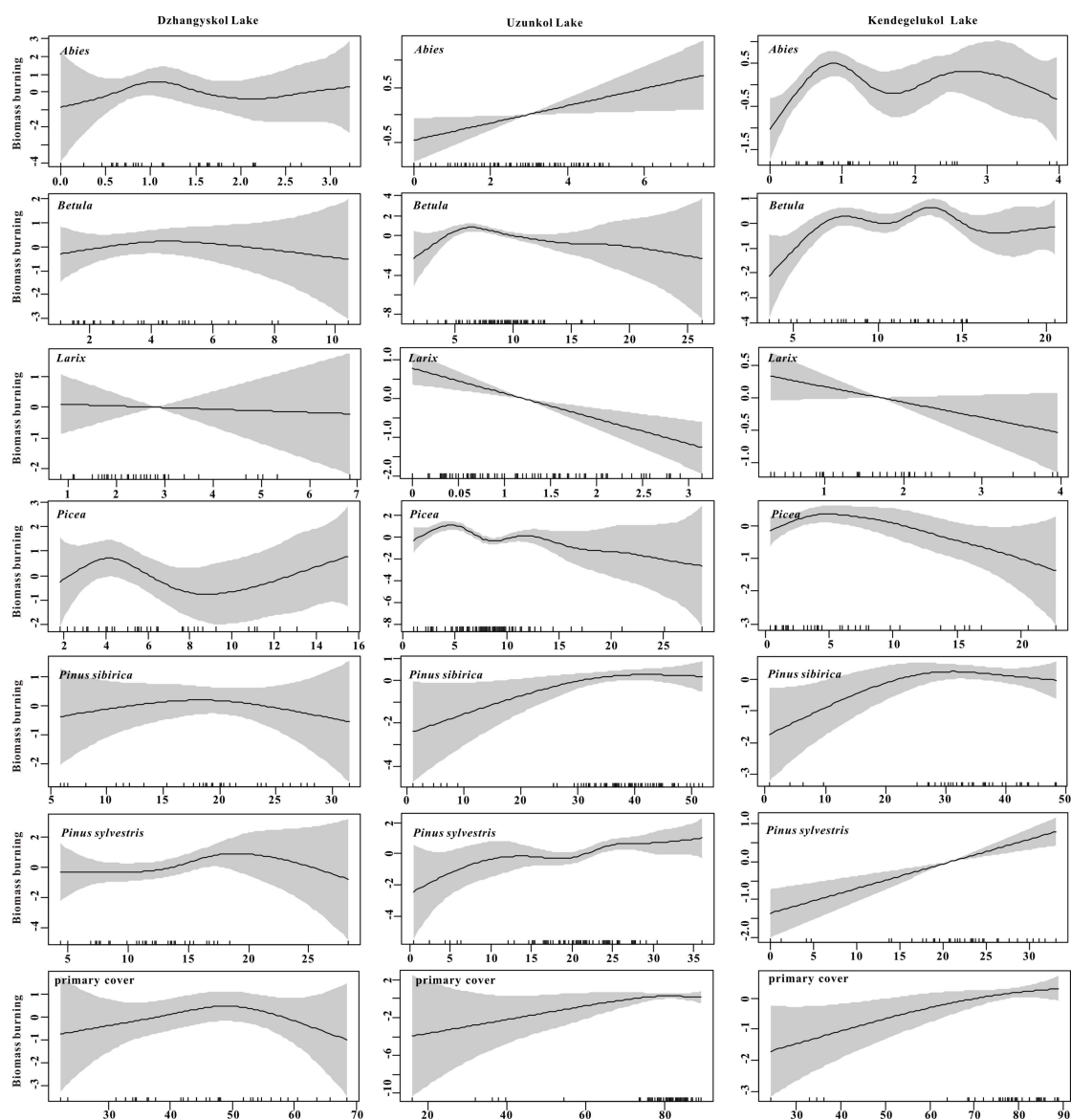


Fig. S5. Generalized Additive Models showing the relationship between biomass burning (y-axis) and dominant drivers (*Abies*, *Betula*, *Larix*, *Picea*, *Pinus sibirica*, *Pinus sylvestris* and primary forest cover) in Dzhangyskol Lake, Uzunkol Lake and Kendegetukol Lake. Pointwise confidence intervals (95%) are indicated by the gray bands.

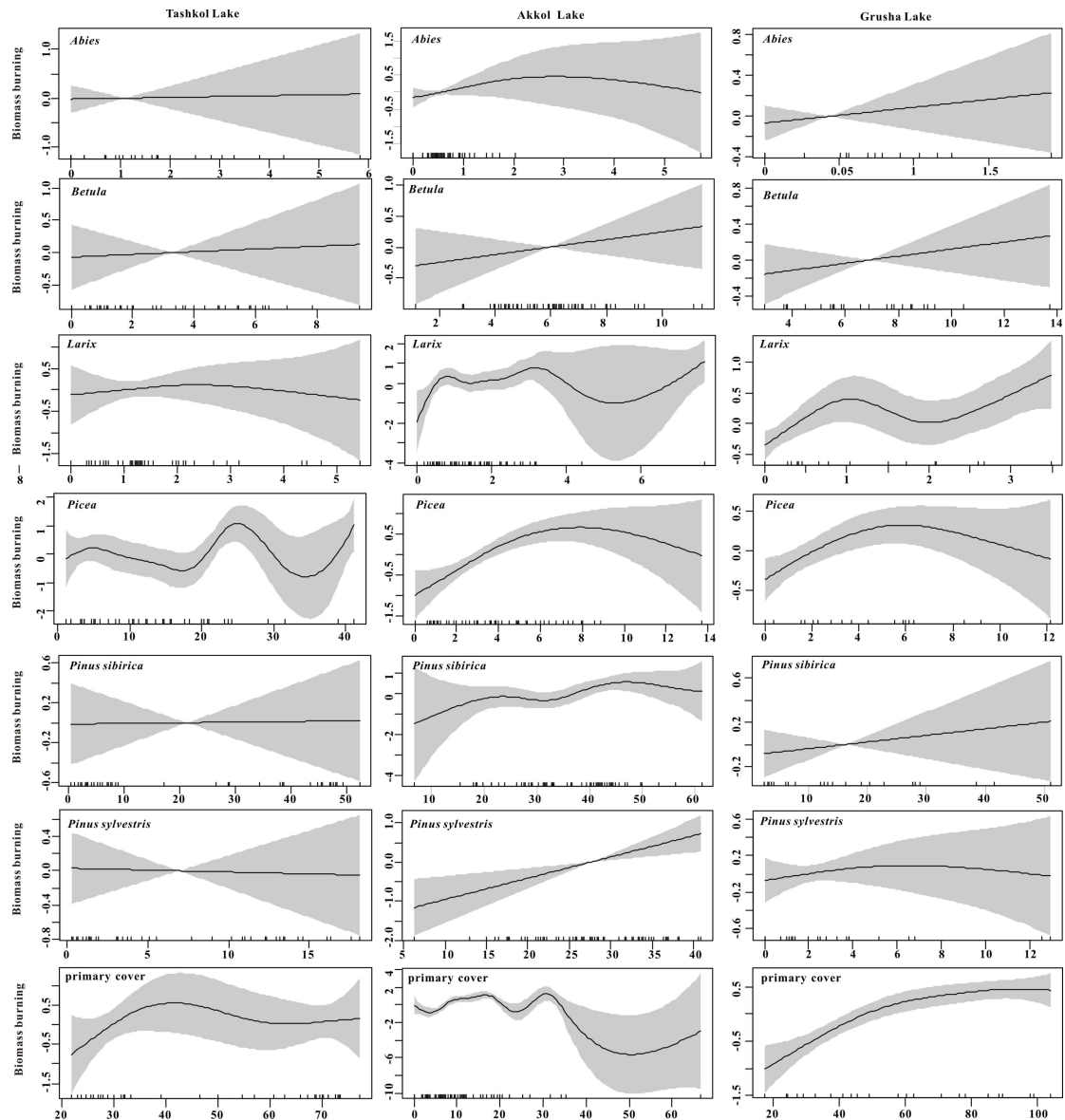


Fig. S6. Generalized Additive Models showing the relationship between biomass burning (y-axis) and dominant drivers (*Abies*, *Betula*, *Larix*, *Picea*, *Pinus sibirica*, *Pinus sylvestris* and primary forest cover) in Tashkol Lake, Akkol Lake and Grusha Lake. Pointwise confidence intervals (95%) are indicated by the gray bands.

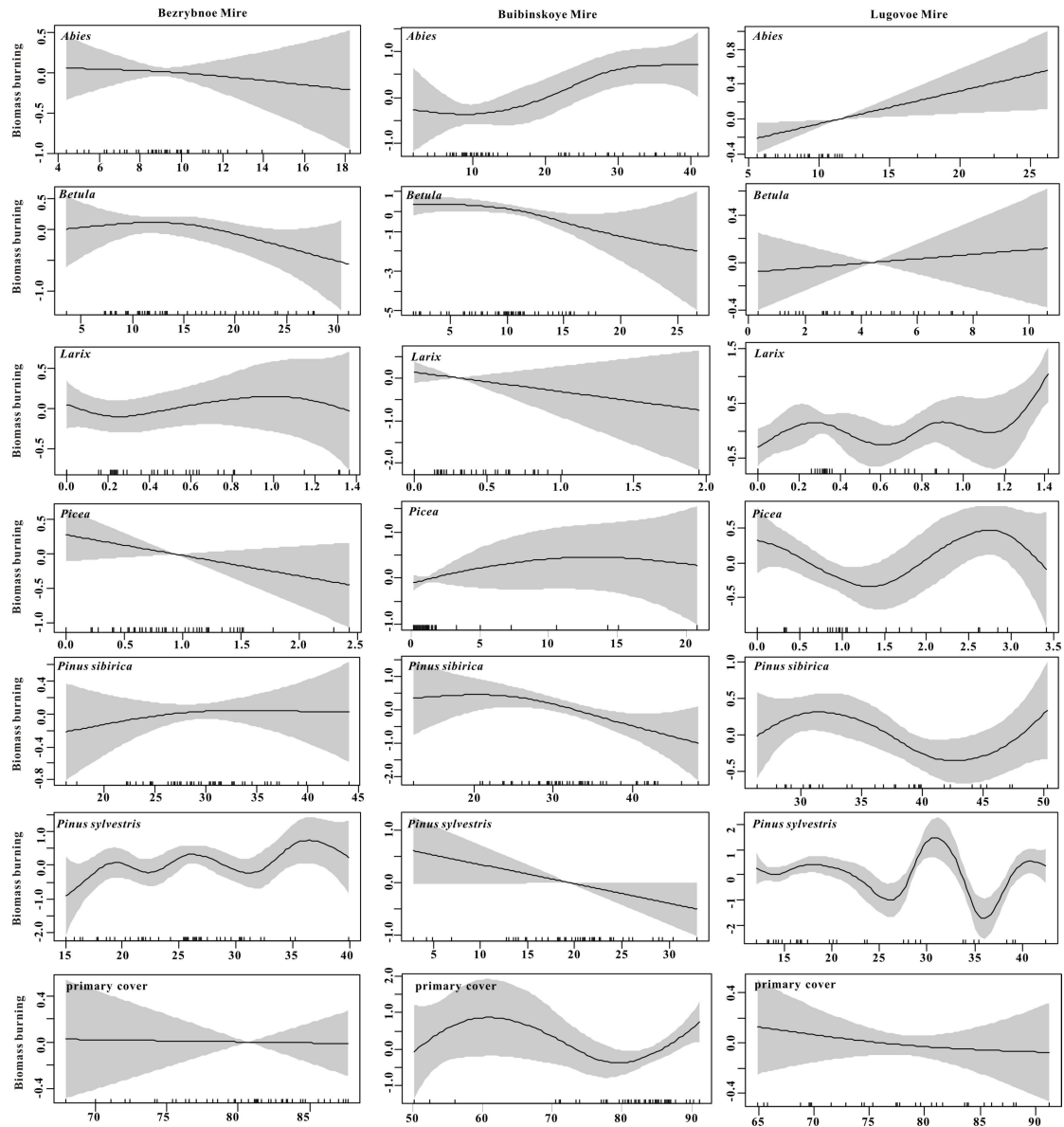


Fig. S7. Generalized Additive Models showing the relationship between biomass burning (y-axis) and dominant drivers (*Abies*, *Betula*, *Larix*, *Picea*, *Pinus sibirica*, *Pinus sylvestris* and primary forest cover) in Buibinskoye Mire, Bezrybnoye Mire and Lugovoe Peat. Pointwise confidence intervals (95%) are indicated by the gray bands.

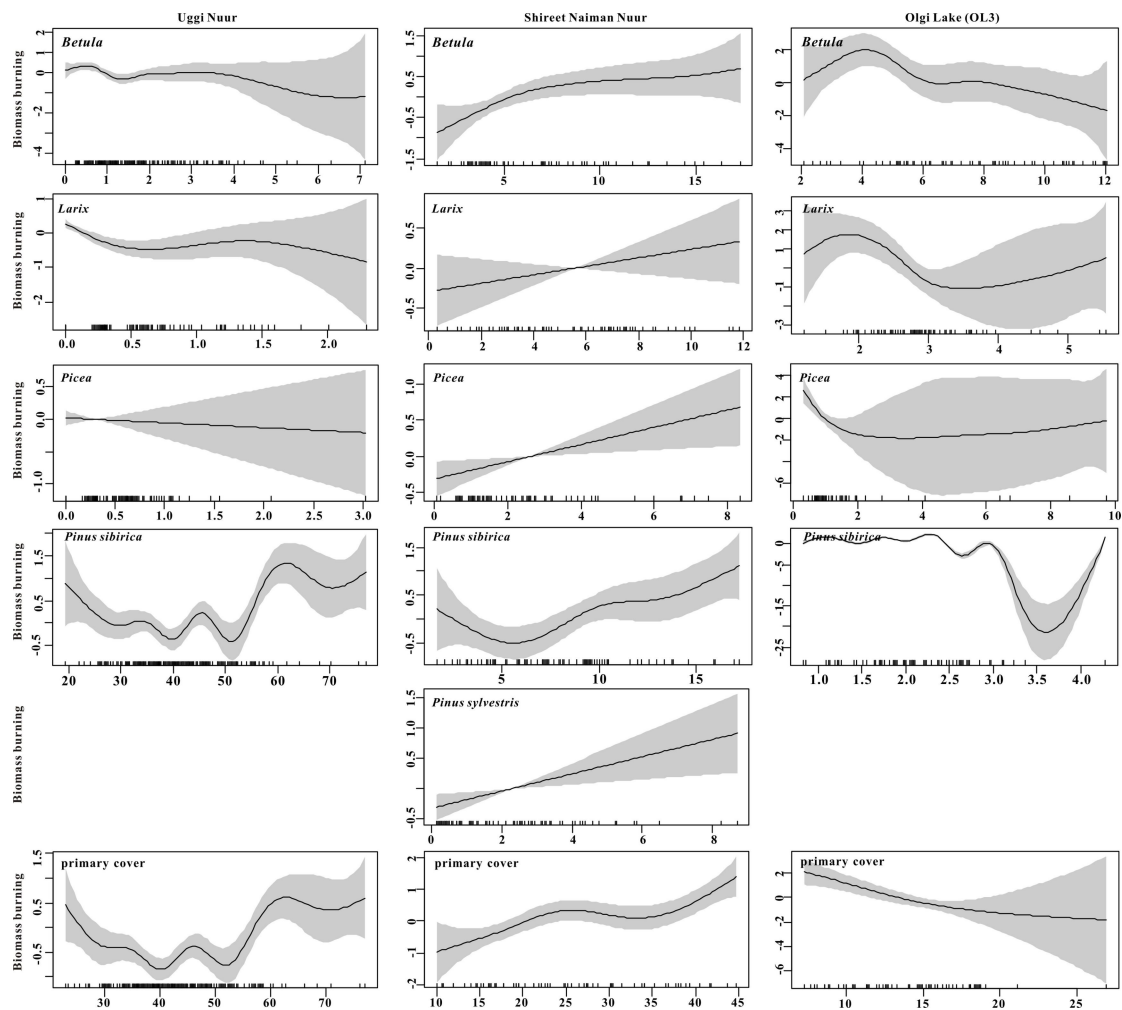


Fig. S8. Generalized Additive Models showing the relationship between biomass burning (y-axis) and dominant drivers (*Abies*, *Betula*, *Larix*, *Picea*, *Pinus sibirica*, *Pinus sylvestris* and primary forest cover) in Olgi Lake(OL3), Shireet Naiman Nuur and Uggi Nuur. Pointwise confidence intervals (95%) are indicated by the gray bands.

References

- Agatova, A.R., Nepop, R.K., Bronnikova, M.A., Slyusarenko, I.Tu., Orlova, L.A. Human occupation of South Eastern Altai highlands (Russia) in the context of Environmental changes. *Archaeological and Anthropological Sciences*. DOI 10.1007/s12520-014-0202-7.
- Barhoumi, C., Bliedtner, M., Zech, R., Behling, H., 2024. Holocene vegetation, fire, climate dynamics and human impact in the upper Orkhon Valley of the Khangai Mountains, Mongolia. *Quat. Sci. Rev.* 334, 108713.
- Barhoumi, C., Bliedtner, M., Zech, R., Behling, H., 2024. Holocene vegetation, fire,

265 climate dynamics and human impact in the upper Orkhon Valley of the Khangai
 266 Mountains, Mongolia. *Quat. Sci. Rev.* 334, 108713.

267 Bezrukova, E.V., Abzaeva, A.A., Letunova, P.P., Kulagina, N.V., Vershinin, A.V.,
 268 Belov, A.V., Orlova, L.A., Danko, L.V., Krapivina, S.M., 2005. Post-glacial
 269 history of Siberian spruce (*Picea obovate*) in the lake Baikal area and the
 270 significance of this species as a paleo-environmental indicator. *Quaternary*
 271 *International* 136, 47-57. DOI: 10.1016/j.quaint.2004.11.007.

272 Blyakharchuk, T.A., Wright, H.E., Borodavko, P.S., van der Knaap, W.O., Ammann,
 273 B., 2004. Late Glacial and Holocene vegetational changes on the Ulagan
 274 high-mountain plateau, Altai Mountains, southern Siberia. *Palaeogeography,*
 275 *Palaeoclimatology, Palaeoecology*, 209(1-4), 259-279.

276 Blyakharchuk, T.A., Wright, H.E., Borodavko, P.S., van der Knaap, W.O., Ammann,
 277 B., 2007. Late glacial and Holocene vegetational history of the Altai mountains
 278 (southwestern Tuva Republic, Siberia). *Palaeogeography, Palaeoclimatology,*
 279 *Palaeoecology*, 245(3-4), 518-534.

280 Blyakharchuk, T.A., Wright, H.E., Borodavko, P.S., van der Knaap, W.O., Ammann,
 281 B., 2008. The role of pingos in the development of the Dzhangyskol lake-pingo
 282 complex, central Altai Mountains, southern Siberia. *Palaeogeography,*
 283 *Palaeoclimatology, Palaeoecology*, 257(4), 404-420.

284 Blyakharchuk, T.A., Chernova, N.A., 2013. Vegetation and climate in the Western
 285 Sayan Mts according to pollen data from Lugovoe Mire as a background for
 286 prehistoric cultural change in southern Middle Siberia. *Quat. Sci. Rev.* 75, 22-42.

287 Blyakharchuk, T.A., Kuryina, I.V., Pologova, N.N., 2019. Late Holocene dynamics of
 288 vegetation cover and climate humidity in the southeastern sector of the West
 289 Siberian Plain according to palynological and rhizopod studies of peat deposits.
 290 *Bulletin of Tomsk State University. Biology* 45, 164–189. (in Russian)

291 Blyakharchuk, T.A., Pupysheva, M.A., 2022. Indication of fires in the thousand-year
 292 history of Central Altai. *Geography and Natural Resource*, 4, 128-136 (In
 293 Russian).

294 Blyakharchuk, T.A., van Hardenbroek, M., Pupysheva, M.A., Kirpotin, S.N.,

295 Blyakharchuk, P.A., 2024. Late Glacial and Holocene history of climate,
 296 vegetation landscapes and fires in South Taiga of Western Siberia based on
 297 radiocarbon dating and multi-proxy palaeoecological research of sediments from
 298 Shchuchye Lake. Radiocarbon, 1-24, doi:10.1017/RDC.2024.103.

299 Blyakharchuk, T.A., 2020. Dynamics of vegetation cover and quantitative
 300 palaeoclimatic reconstructions in the Western Sayan Mountains from the Late
 301 Glacial period to the present time according to a palynological study of the
 302 Yuzhno-Buybinskoe mire. In IOP Conference Series: Earth and Environmental
 303 Science (Vol. 611, No. 1, p. 012026). IOP Publishing.

304 Blaauw, M., Christen, J.A., 2011. Flexible paleoclimate age-depth models using an
 305 autoregressive gamma process. Bayesian Analysis 6, 457–474.

306 Carter, V.A., Bobek, P., Moravcová, A., Šolcová, A., Chiverrell, R.C., Clear, J.L.,
 307 Kuneš, P., 2020. The role of climate-fuel feedbacks on Holocene biomass
 308 burning in upper-montane Carpathian forests. Global and Planetary Change, 193,
 309 103264.

310 Feurdean, A., Florescu, G., Tanțău, I., Vannière, B., Diaconu, A. C., Pfeiffer, M.,
 311 Kirpotin, S., 2020. Recent fire regime in the southern boreal forests of western
 312 Siberia is unprecedented in the last five millennia. Quat. Sci. Rev. 244, 106495.

313 Feurdean, A., Diaconu, A.C., Pfeiffer, M., Gałka, M., Hutchinson, S.M., Butiseaca, G.,
 314 Gorina, N., Tonlkov, S., Niamir, A., Tantau, I., Zhang, H., Kirpotin S., 2022.
 315 Holocene wildfire regimes in Western Siberia: Interaction between peatland
 316 moisture conditions and the composition of plant functional types. Climate of the
 317 Past 18, 1255–1274.

318 Fu, B.J., Liu, G.H., Ouyang, Z.Y., 2013. Ecological regionalization in China. Beijing:
 319 Science Press.

320 Kasischke, E.S., 2000. Boreal ecosystems in the global carbon cycle. In: Kasischke,
 321 E.S., Stocks, B.J. (Eds.), Fire, Climate Change, and Carbon Cycling in the Boreal
 322 Forest. Ecological.

323 Kelly, R.F., Higuera, P.E., Barrett, C.M., Hu, F.S., 2011. A signal-to-noise index to
 324 quantify the potential for peak detection in sediment–charcoal records. Quat. Res.

75, 11–17.

Khabarov, N., Krasovskii, A., Obersteiner, M., Swart, R., Dosio, A., San-Miguel-Ayanz, J., Migliavacca, M., 2016. Forest fires and adaptation options in Europe. *Region. Environ. Chang.* 16, 21–30.

Goldammer, J.G., Furyaev, V., 2013. Fire in ecosystems of boreal Eurasia (Vol. 48). Springer Science & Business Media.

Hastie, T.J., Tibshirani, R.J., 1986. Generalized additive models. *Stat. Sci.* 1 (3), 297–318.

Higuera, P.E., Brubaker, L.B., Anderson, P.M., Hu, F.S., Brown, T., 2009. Vegetation mediated the impacts of postglacial climate change on fire regimes in the south Central Brooks Range, Alaska. *Ecol. Monogr.* 79, 201–219.

Higuera, P.E., Gavin, D.G., Bartlein, P.J., Hallett, D.J., 2010. Peak detection in sediment–charcoal records: impacts of alternative data analysis methods on fire-history interpretations. *Int. J. Wildland Fire* 19, 996–1114.

Hu, Y., Huang, X., Demberel, O., Zhang, Jun, Xiang, L., Gundegmaa, V., Huang, C., Zheng, M., Zhang, Jiawu, Qiang, M., Xiao, J., Chen, F., 2024. Quantitative reconstruction of precipitation changes in the Mongolian Altai Mountains since 13.7 ka. *Catena* 234, 107536.

Huang, X., Peng, W., Rudaya, N., Grimm, E.C., Chen, X., Cao, X., Zhang, J., Pan, X., Liu, S., Chen, C., Chen, F., 2018. Holocene vegetation and climate dynamics in the Altai Mountains and surrounding areas. *Geophys. Res. Lett.* 45 (13), 6628–6636.

Lézine, A.M., Izumi, K., Achoundong, G., 2023. Mbi Crater (Cameroon) illustrates the relations between mountain and lowland forests over the past 15,000 years in western equatorial Africa. *Quat. Int.* 657, 67–76.

Li, Y., Zhang, Y., Wang, J., Wang, L., Li, Y., Chen, L., Zhao, L., Kong, Z., 2019. Preliminary study on pollen, charcoal records and environmental evolution of Alahake Saline Lake in Xinjiang since 4,700 cal yr BP. *Quat. Int.* 513, 8–17.

Li, Y., Zhang, D., Zhang, Y., Sun, A., Li, X., Huang, X., Zhang, Y., Li, Y., 2024. Distentangling the late-Holocene human–environment interactions in the Altai Mountains within the Arid Central Asia. *Palaeogeo. Palaeoclimat. Palaeoeco.*

654, 112466.

Moritz, M.A., Batllori, E., Bradstock, R.A., Gill, A.M., Handmer, J., Hessburg, P.F., Leonard, J., McCaffrey, S., Odion, D.C., Schonennagel, T., Syphard, A.D., 2014. Learning to coexist with wildfire. *Nature*, 515(7525), 58-66.

Power, M.J., Marlon, J., Ortiz, N., et al., 2007. Changes in fire regimes since the Last Glacial Maximum: an assessment based on a global synthesis and analysis of charcoal data. *Climate dynamics*, 30, 887-907.

Pupychева, M.A., Blyakharchuk, T.A., 2024. Late Holocene dynamics of fires in the forest-steppe zone (a case study of the Nikolaevsky Ryam) *Geografiya I prirosnye resursy*. 1, 54-61 (in Russian).

Reimer, P.J., Austin, W.E., Bard, E., Bayliss, A., Blackwell, P.G., Ramsey, C.B., Talamo, S., 2020. The IntCal20 Northern Hemisphere radiocarbon age calibration curve (0–55 cal kBP). *Radiocarbon* 62 (4), 725–757.

Rudaya, N., Sergey, K., Michał, S., Xianyong, C., Snezhana, Z., 2020. Postglacial history of the steppe Altai: climate, fire and plant diversity. *Quat. Sci. Rev.* 249, 106616.

Sun, A., Feng, Z.D., Ran, M., Zhang, C.J., 2013. Pollen-recorded bioclimatic variations of the last ~22,600 years retrieved from Achit Nuur core in the western Mongolian Plateau. *Quat. Int.* 311, 36-43.

Stockmarr J.A., 1971. Tabletes with spores used in absolute pollen analysis. *Pollen spores*, 13, 61-621.

Umbanhowar Jr, C.E., Shinneman, A.L., Tserenkhand, G., Hammon, E.R., Lor, P., Nail, K., 2009. Regional fire history based on charcoal analysis of sediments from nine lakes in western Mongolia. *Holocene* 19(4), 611-624.

Unkelbach, J., Dulamsuren, C., Klinge, M., Behling, H., 2021. Holocene high-resolution forest-steppe and environmental dynamics in the Tarvagatai Mountains, northcentral Mongolia, over the last 9570 cal yr BP. *Quat. Sci. Rev.* 266, 107076.

Walker, X.J., Baltzer, J.L., Cumming, S.G., Day, N.J., Ebert, C., Goetz, S., Johnstone, J.F., Potter, S., Rogers, B.M., Schuur, E.A.G., Turetsky, M.R., Mack, M.C., 2019. Increasing wildfires threaten historic carbon sink of boreal forest soils. *Nature*,

387 572, 520-523.

388 Wang, W., Ma, Y.Z., Feng, Z.D., Narantsetseg, Ts, Liu, K.B., Zhai, X.W., 2011. A
389 prolonged dry mid-Holocene climate revealed by pollen and diatom records from
390 Lake Ugi Nuur in central Mongolia. *Quat. Int.* 229 (1e2), 74-83.

391 Wood, S.N., 2017. *Generalized Additive Models: An Introduction with R* (2nd
392 Edition). Chapman and Hall/CRC, pp1-476.
393